Lee et al. *Experimental & Molecular Medicine* (2018) 50:48
DOI 10.1038/s12276-018-0074-5

Experimental & Molecular Medicine

ARTICLE Open Access

Altered AKAP12 expression in portal fibroblasts and liver sinusoids mediates transition from hepatic fibrogenesis to fibrosis resolution

Hye Shin Lee[1], Jinhyeok Choi[1], Taekwon Son[1], Hee-Jun Wee[1], Sung-Jin Bae[1], Ji Hae Seo[2], Ji Hyun Park[1], Soo Hyung Ryu[3], Danbi Lee[4], Myoung Kuk Jang[5], Eunsil Yu[6], Young-Hwa Chung[4] and Kyu-Won Kim[1,7]

Abstract

Liver fibrosis can be reversed by removing its causative injuries; however, the molecular mechanisms mediating the resolution of liver fibrogenesis are poorly understood. We investigate the role of a scaffold protein, A-Kinase Anchoring Protein 12 (AKAP12), during liver fibrosis onset, and resolution. Biliary fibrogenesis and fibrosis resolution was induced in wild-type (WT) or AKAP12-deficient C57BL/6 mice through different feeding regimens with 0.1% 3,5-diethoxycarbonyl-1,4-dihydrocollidine (DDC)-containing chow. AKAP12 expression in portal fibroblasts (PFs) and liver sinusoidal endothelial cells (LSECs) gradually decreased as fibrosis progressed but was restored after cessation of the fibrotic challenge. Histological analysis of human liver specimens with varying degrees of fibrosis of different etiologies revealed that AKAP12 expression diminishes in hepatic fibrosis from its early stages onward. AKAP12 KO mice displayed reduced fibrosis resolution in a DDC-induced biliary fibrosis model, which was accompanied by impaired normalization of myofibroblasts and capillarized sinusoids. RNA sequencing of the liver transcriptome revealed that genes related to ECM accumulation and vascular remodeling were mostly elevated in AKAP12 KO samples. Gene ontology (GO) and bioinformatic pathway analyses identified that the differentially expressed genes were significantly enriched in GO categories and pathways, such as the adenosine 3′,5′-cyclic monophosphate (cAMP) pathway. Knockdown of the AKAP12 gene in cultured primary PFs revealed that AKAP12 inhibited PF activation in association with the adenosine 3′,5′-cyclic monophosphate (cAMP) pathway. Moreover, AKAP12 knockdown in LSECs led to enhanced angiogenesis, endothelin-1 expression and alterations in laminin composition. Collectively, this study demonstrates that AKAP12-mediated regulation of PFs and LSECs has a central role in resolving hepatic fibrosis.

Introduction

Liver fibrosis is the final outcome of chronic hepatic damage caused by multiple etiologies, such as virus infections, alcohol over-consumption, and autoimmune or metabolic diseases[1,2]. In cirrhosis—the end stage of liver fibrosis—liver malfunction with severe complications arises due to the distortion of liver architecture caused by aberrant extracellular matrix (ECM) deposition. However, an important characteristic of liver fibrosis that can provide new therapeutic strategies is its reversibility, even at an advanced stage, upon removal of the causative injury[3,4].

Hepatic non-parenchymal cells are involved not only in fibrogenesis but also in fibrosis resolution. Hepatic stellate cells (HSCs) and portal fibroblasts (PFs) are mesenchymal cells capable of transforming into myofibroblasts that

Correspondence: K-W. Kim (qwonkim@snu.ac.kr)
[1]College of Pharmacy and Research, Institute of Pharmaceutical Sciences Seoul National University Seoul 08826, Korea
[2]Department of Biochemistry, School of Medicine, Keimyung University, Daegu 42601, Korea
Full list of author information is available at the end of the article

aberrantly produce ECM proteins under fibrogenic conditions[2,5]. These cells are removed by apoptosis[6] or senescence[7] during fibrosis resolution; however, some remain in a quiescent state[8]. The molecular mechanisms underlying the transition from fibrogenesis to fibrosis resolution are not fully understood; however, shifting the balance between pro-fibrotic pathways, such as TGF-β1 and PDGF signaling[9,10], and anti-fibrotic ones, such as peroxisome proliferator-activated receptor gamma (PPARγ) and cAMP pathways[11–13], may mediate this transition.

Under fibrotic conditions, liver sinusoids undergo vascular remodeling, which includes angiogenesis and capillarization characterized by the loss of fenestrae and the formation of basement membrane[14]. As differentiated liver sinusoidal endothelial cells (LSECs) function to maintain the quiescent status of HSCs, loss of LSEC differentiation under fibrosis contributes to HSC activation[15,16]. Forced re-differentiation of LSECs by a soluble guanylate cyclase activator promotes fibrosis regression in rodent models[17], suggesting that the normalization of LSECs to their differentiated state is a prerequisite for proper liver fibrosis resolution.

AKAP12 is a scaffold protein known to integrate effector proteins such as protein kinase A, protein kinase C, and protein phosphatase 2B for the β-adrenergic receptor pathway, through which it has a role in regulating cAMP compartmentalization and the re-sensitization of β-adrenergic receptors[18,19]. As AKAP12 is widely expressed by several cell types, it is reported to have diverse physiological functions, such as inhibition of angiogenesis[20], promotion of meningeal reconstruction[21,22], and tumor suppression[23]. In connection to chronic liver diseases, AKAP12 is reported to be down-regulated by an epigenetic mechanism in human hepatocellular carcinoma[24]. However, little is known regarding its expression and function in normal and fibrotic livers.

In this study, we aim to investigate the molecular mechanisms by which non-parenchymal cells—in particular, PFs and LSECs—modulate hepatic fibrosis resolution. By examining the expression profiles of AKAP12 in normal and fibrotic livers, we investigate the role of this protein in hepatic fibrogenesis and fibrosis resolution.

Materials and methods

Animals and fibrosis induction

All mouse experiments were reviewed and approved by the Committee for Care and Use of Laboratory Animals at Seoul National University according to the Guide for Animal Experiments edited by the Korean Academy for Medical Sciences. Wild-type (WT) and AKAP12-deficient (AKAP12 KO) C57BL/6 mice were bred and maintained as described previously[25]. Hepatic fibrosis was induced by feeding mice a 3,5-diethoxycarbonyl-1,4-dihydrocollidine (DDC)-supplemented diet; 0.1% DDC (Sigma) was mixed with normal mouse chow and fed to weight-matched 8- to 10-week-old male mice. The mice were kept on the DDC diet for 3 weeks, following which they were returned to a normal diet for the next 2 weeks. At the end of the experimental period, the mice were killed via deep anesthesia and killed by cardiac perfusion.

Human tissue specimens

Tissues from normal and fibrotic human livers were obtained through biopsy specimens from patients who visited the Asan Medical Center, University of Ulsan, College of Medicine, Seoul, Korea, for diagnosis. Informed consent was obtained from all patients. The patients' clinical characteristics are summarized in supplementary Table 1. Fibrosis grades were determined by gross and microscopic examination of the liver tissues. The study was approved by the Institutional Review Board of the Asan Medical Center, Seoul, Korea.

Histological analysis and immunohistochemistry

Immunofluorescence staining was performed on paraffin sections or frozen sections. The paraffin sections were de-paraffinized and stained with Picro-Sirius Red (Abcam, Cambridge, MA, USA) according to the manufacturer's instructions to visualize the deposition of ECM proteins. To stain the paraffin sections, antigen retrieval was conducted for 30 min at 95 °C in Tris or citrate buffer, depending on antibody compatibility. After blocking with 5% normal donkey serum (Sigma-Aldrich) in PBS solution, the sections were incubated overnight at 4 °C with primary antibodies for AKAP12 (I. Gelman, Roswell Park Cancer Institute), aSMA (Dako), laminin (Sigma), SE-1 (R&D Systems), CD31 (BD Biosciences), Thy-1 (BD Biosciences), collagen I (Southern Biotech), collagen III (Southern Biotech), Desmin (R&D Systems), VEGFR2 (Cell Signaling), F4/80 (Abcam), SE-1 (R&D Systems), and collagen IV (Southern Biotech). After extensive washing in PBS containing 0.1% Tween-20 solution, the sections were treated with Alexa 488- or 546-conjugated secondary antibodies (1:750, Invitrogen, Carlsbad, CA, USA) for 1 h at room temperature followed by counter staining with Hoechst (Sigma). Fluorescent images were taken under a confocal microscope (Carl Zeiss AG, Oberkochen, Germany), and immuno-positive areas were quantified by ImageJ software. Unless specified otherwise, 5–10 images from a single animal were quantified, and the mean value was considered to be a representative value for the animal.

RNA isolation and qPCR

Liver tissues were incubated in Trizol Reagent (Invitrogen) for 5 min, followed by homogenization using TissueLyser II (Qiagen, Hilden, Germany), and total RNA

was extracted according to the manufacturer's instructions. Two micrograms of RNA from each sample was reverse-transcribed with Moloney murine leukemia virus (MMLV) reverse transcriptase (Promega Corp., Madison, WI, USA). Quantitative real-time PCR was then performed using a StepOnePlus Real-Time PCR system (Applied Biosystems, Foster city, CA, USA) with a Real-Helix qPCR kit (NanoHelix, Seoul, Korea). The relative mRNA levels were normalized using housekeeping genes, such as GAPDH, TBP, and 18S rRNA. The primer sequences used in this study are provided in Supplementary Table 2.

Cell culture and transfection

Primary human liver sinusoidal endothelial cells (hLSECs, Cell Biologics, Chicago, IL, USA) were maintained in complete human endothelial medium (Cell Biologics). Cells were transfected with control or SMARTpool siRNAs against human AKAP12 (GE Dharmacon) at passages 5 to 7 using oligofectamine transfection reagent (Invitrogen). Primary mouse portal fibroblasts were cultured using the biliary tree expansion method after intrahepatic collagenase perfusion as described previously[26]. Control or SMARTpool siRNAs against mouse AKAP12 (GE Dharmacon) were transfected at passages 1 to 2 using JetPrime transfection reagent (Polyplus transfection, Strasbourg, France).

mRNA sequencing analysis

Total RNA was isolated from mouse liver tissue using TRIzol® RNA Isolation Reagents (Life technologies, Carlsbad, CA). RNA integrity was confirmed by a bioanalyzer using an Agilent RNA 6000 Pico Kit (Agilent, Santa Clara, CA). The isolated total RNA was processed for preparing a mRNA sequencing library using a TruSeq stranded mRNA sample preparation kit (Illumina, San Diego, CA) according to the manufacturer's instructions. Briefly, mRNA was isolated from 400 ng of total RNA using RNA purification beads for polyA capture, followed by enzymatic shearing. After first and second strand cDNA synthesis, A-tailing and end repair were performed for ligation of the proprietary primers, which incorporated unique sequencing adaptors with an index for tracking Illumina reads from multiplexed samples run on a single sequencing lane. For each library, an insert size of ~220 bp was confirmed by Bioanalyzer using an Agilent DNA Kit (Agilent, Santa Clara, CA), and quantification of library was measured by real-time PCR using a CFX96 real-time system (BioRad, Hercules, CA). Samples were sequenced with the Illumina NextSeq 500 platform with paired-end, 75-bp reads for mRNA-seq using a NextSeq 500/550 High Output Kit version 2 (for 150 cycles). Raw image data were transformed by base-calling into sequence data and stored in FASTQ format.

Trimming, alignment, and expression analysis

Three paired-end 75 bp reads from three replicates each of wild-type mouse sample and AKAP12 knock out mouse sample were trimmed for both PCR and sequencing adapters with Cutadapt. Trimmed reads were aligned to the mm10 mouse reference genome using STAR[27]. Quantification of gene expression was performed with Cufflinks to calculate FPKM values[28].

Differential expression analysis

Significant differential expression was analyzed using edgeR[29] at the gene level. A heatmap for differentially expressed genes was generated using R language. Functional classification was performed using DAVID[30].

Gene set enrichment analysis

Gene set enrichment analysis (GSEA) was used to determine the extent to which expression profiles were enriched for a priori defined sets of genes from biologically coherent pathways[31]. GSEA was performed using version 2.2 of GSEA run on all gene sets in version 5.2 of the Molecular Signatures Database to correct for multiple hypotheses testing; the FDR threshold was set at ≤0.25.

Statistical analysis

All data are expressed as the mean ± SEM. One-way ANOVA, followed by Tukey's tests or two-tailed Student's *t*-tests, was used for statistical analyses. Differences between groups were considered significant for P 0.05. All statistical analyses were performed using GraphPad Prism V.5.00 (GraphPad Software, San Diego, California, USA).

Data availability

The RNA-seq data are publicly available through the National Center for Biotechnology Information's Gene Expression Omnibus under accession number GSE104030.

Results

Expression patterns of AKAP12 in normal and fibrotic mouse livers

Immunofluorescence staining of normal mouse liver tissues showed that AKAP12 was expressed along the endothelium and in cells surrounding the portal tract but not in the central vein (Fig. 1a). Double immunofluorescence staining identified AKAP12-expressing cells in the portal tract as PFs as the AKAP12 signal merged with the PF markers thy-1 (Fig. 1b, upper row), desmin, and PDGFRα but not with EpCAM or CD31 (Supplementary Figure 1a). Interestingly, AKAP12-positive cells in the liver parenchyma were LSECs, as revealed by colocalization of AKAP12 with SE-1 signals (Fig. 1b, bottom row) and sinusoidal basement membrane marker collagen type IV (Supplementary Figure 1b). Desmin-

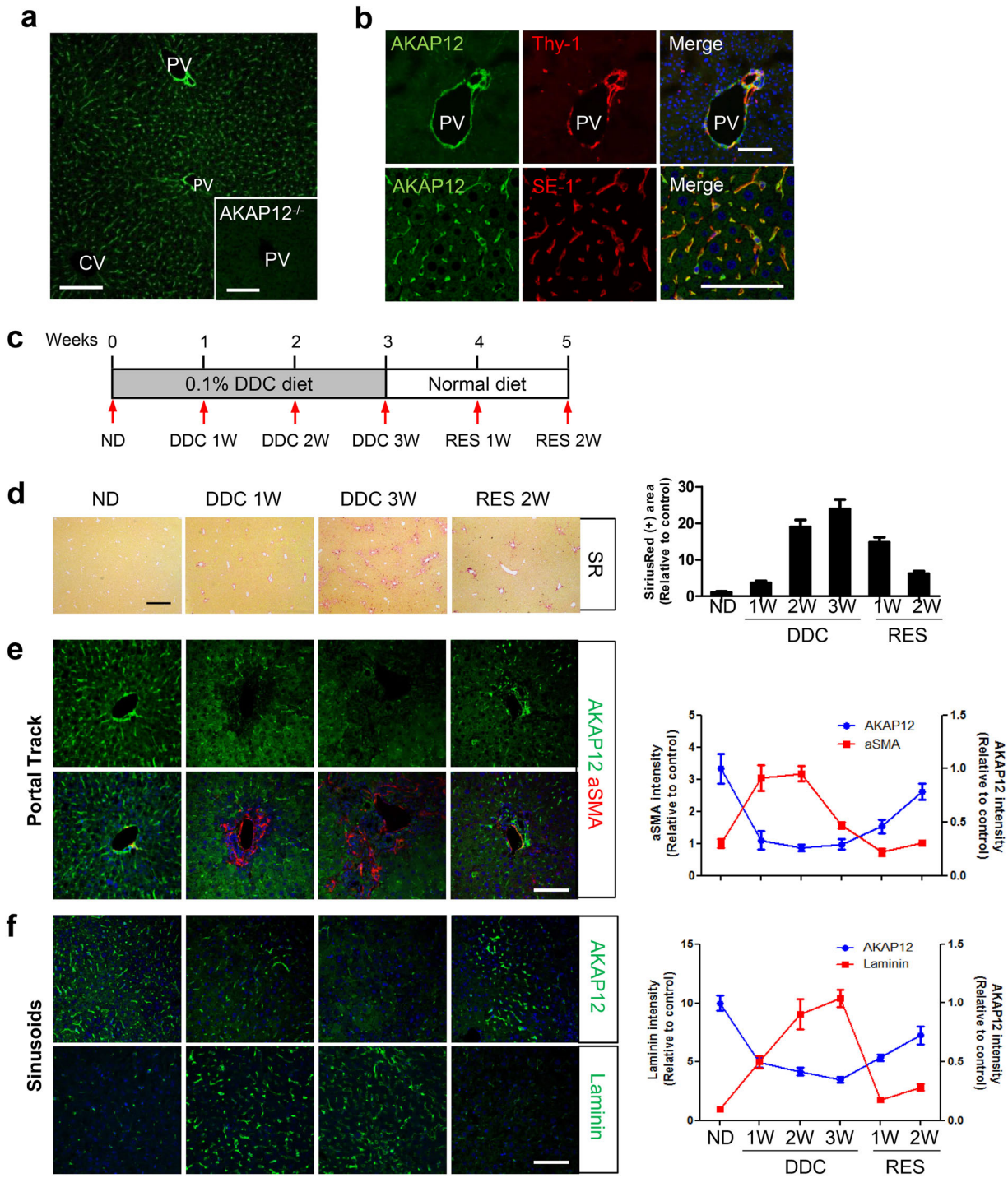

Fig. 1 AKAP12 is mainly expressed in PFs and LSECs of normal liver, and its expression is dynamically altered during fibrosis progression and resolution. a Paraffin sections from normal WT livers were subjected to immunofluorescence staining for AKAP12 (green). Note the specific immunoreactivity around the portal vein and liver sinusoids, which was not detected in AKAP12 KO livers (inlet). PV portal vein, CV central vein. **b** Double immunostaining of liver sections from WT mice for AKAP12 and other cell-type markers. AKAP12(+) cells in the portal tract are shown merged with thy-1(+) PFs, and AKAP12(+) cells in the liver parenchyma are shown merged with SE-1(+) LSECs. **c**–**e** Mice fed a normal diet (ND) or DDC-containing diet for 1–3 weeks (DDC 1–3W) or DDC diet for 3 weeks followed by a normal diet for 1–2 weeks (RES 1, 2W) (**c**). Liver sections from each experimental group stained with Sirius Red (**d**), AKAP12 and αSMA (**e**), and AKAP12 or laminin (**f**). Graphs show morphometric quantification of staining-positive areas relative to control liver sections. Data are expressed as the mean ± SEM. $n = 7–9$ per group. Scale bars represent 100 μm in **a**, **b**, **e**, and **f**, and 500 μm in **d**

positive HSCs were in close proximity to AKAP12-positive cells, but they rarely overlapped (Supplementary Figure 1b). The livers of AKAP12 KO mice exhibited disorganized sieve plates with a ~25% reduction in the number of fenestrae per unit area (Supplementary Figure 2a). However, under normal circumstances, we found no indication of liver disease or histological/functional changes due to the AKAP12 gene (data not shown). To investigate the role of AKAP12 in hepatic fibrosis, we used a biliary fibrosis model induced by DDC-feeding. Aberrant ECM accumulation was induced after 3 weeks of DDC-feeding, by which time AKAP12 expression drastically decreased in both PFs and LSECs (Supplementary Figure 2b and c). We then investigated the course of fibrogenesis and fibrosis resolution by feeding mice a DDC diet for 3 weeks, followed by feeding them a normal diet for 2 weeks (Fig. 1c). ECM accumulation, which was observed from the first week of DDC-feeding, gradually increased until the third week. Fibrosis resolution began as soon as the mice began feeding on a normal diet; regression in ECM deposition was clearly evident by the second week of fibrosis resolution (Fig. 1d). AKAP12 expression in the portal tract and sinusoids decreased sharply from the first week of DDC-feeding but was restored during fibrosis resolution (with the removal of DDC-induced injury), even reaching up to 80% of its normal level after 2 weeks of fibrosis resolution (Fig. 1e, f). These data indicate that AKAP12 expression in PFs and LSECs in the liver is dynamically altered during fibrogenesis and fibrosis resolution.

Expression patterns of AKAP12 in normal and fibrotic human livers

Immunohistochemical analyses were used to detect AKAP12 in normal and fibrotic human liver specimens to understand its correlation with human liver conditions. In normal human livers, AKAP12 immunoreactivity was prominent along liver sinusoids and the areas surrounding the portal tract (Fig. 2a), analogous to its expression profile in normal mouse livers. We then analyzed human liver samples with fibrosis caused by three different etiologies, namely, hepatitis B virus (HBV), hepatitis C virus (HCV), and NBNC (non-HBV/non-HCV). Fibrosis grading into stage 1 (portal fibrosis), stage 2 (periportal fibrosis), stage 3 (septal fibrosis), and stage 4 (cirrhosis) was done by pathologists. Liver tissues from a total of 28 patients—4 samples with normal liver histology and 2 samples for each stage of hepatic fibrosis caused by each etiology mentioned previously—were subjected to immunostaining for AKAP12. Intriguingly, AKAP12 immunoreactivity was greatly reduced, even at the early stages of fibrosis (stage 1), irrespective of etiology (Fig. 2b). The average AKAP12-positive area in fibrotic liver samples relative to normal liver samples was the lowest in HBV-induced fibrosis, but the differences among the various etiologies were not statistically significant (Fig. 2c). Besides this, although the mean AKAP12-positive area was the smallest in cirrhotic livers (stage 4), the differences among the various stages were not statistically significant (Fig. 2d). These results suggest that the AKAP12 gene is an early responder to fibrotic changes caused by a wide range of hepatic injuries and that it is involved in the pathogenesis of human liver fibrosis.

Effect of AKAP12 deficiency on DDC-induced liver fibrosis and fibrosis resolution

To investigate the role of AKAP12 in fibrosis progression, we examined the degree of fibrosis in WT and AKAP12 KO mice in response to a DDC challenge; afterwards, we also studied fibrosis resolution after the removal of the DDC challenge. Comparisons of ECM deposition levels after 3 weeks of DDC-feeding showed no significant differences between WT and AKAP12 KO livers (Fig. 3a). However, AKAP12 KO mice displayed reduced fibrosis resolution after being shifted to a normal DDC-free diet for 2 weeks, as revealed by Sirius Red (Fig. 3a), collagen I (Fig. 3b), and collagen III staining (Fig. 3c). Reductions in fibrosis-related ECM gene expression during fibrosis resolution were more apparent than histological regression (Fig. 3d), suggesting that most of the ECM-producing cells were either removed or returned to their quiescent state. In contrast, mRNA levels of these ECM components were approximately two- to threefold higher in AKAP12 KO mice than in WT mice during fibrosis resolution (Fig. 3d). Despite impaired fibrosis resolution in AKAP12 KO mice, the serum levels of liver enzymes returned to normal 2 weeks after the mice were shifted to a normal diet (Supplementary Figure 3).

On the basis of the expression patterns of AKAP12 and the lower levels of fibrosis resolution observed in AKAP12 KO mice, we hypothesized that the restoration of AKAP12 expression during fibrosis resolution led to the deactivation of myofibroblasts and normalization of remodeled sinusoids. Although the population of desmin-positive myofibroblasts grew in the portal area during fibrogenesis and then decreased during fibrosis resolution in WT mice, a significant number of desmin-positive myofibroblasts remained in the livers of AKAP12 KO mice during fibrosis resolution (Fig. 3e). Vascular remodeling, which includes angiogenesis and capillarization of sinusoids, is characteristic of hepatic fibrosis irrespective of etiology[14,32]. DDC-induced fibrosis also led to aberrant angiogenesis within the fibrotic area, as revealed by VEGFR2 staining (Fig. 3f). Furthermore, DDC-induced liver injury led to the formation of a sinusoidal basement membrane as revealed by laminin staining (Fig. 3e).

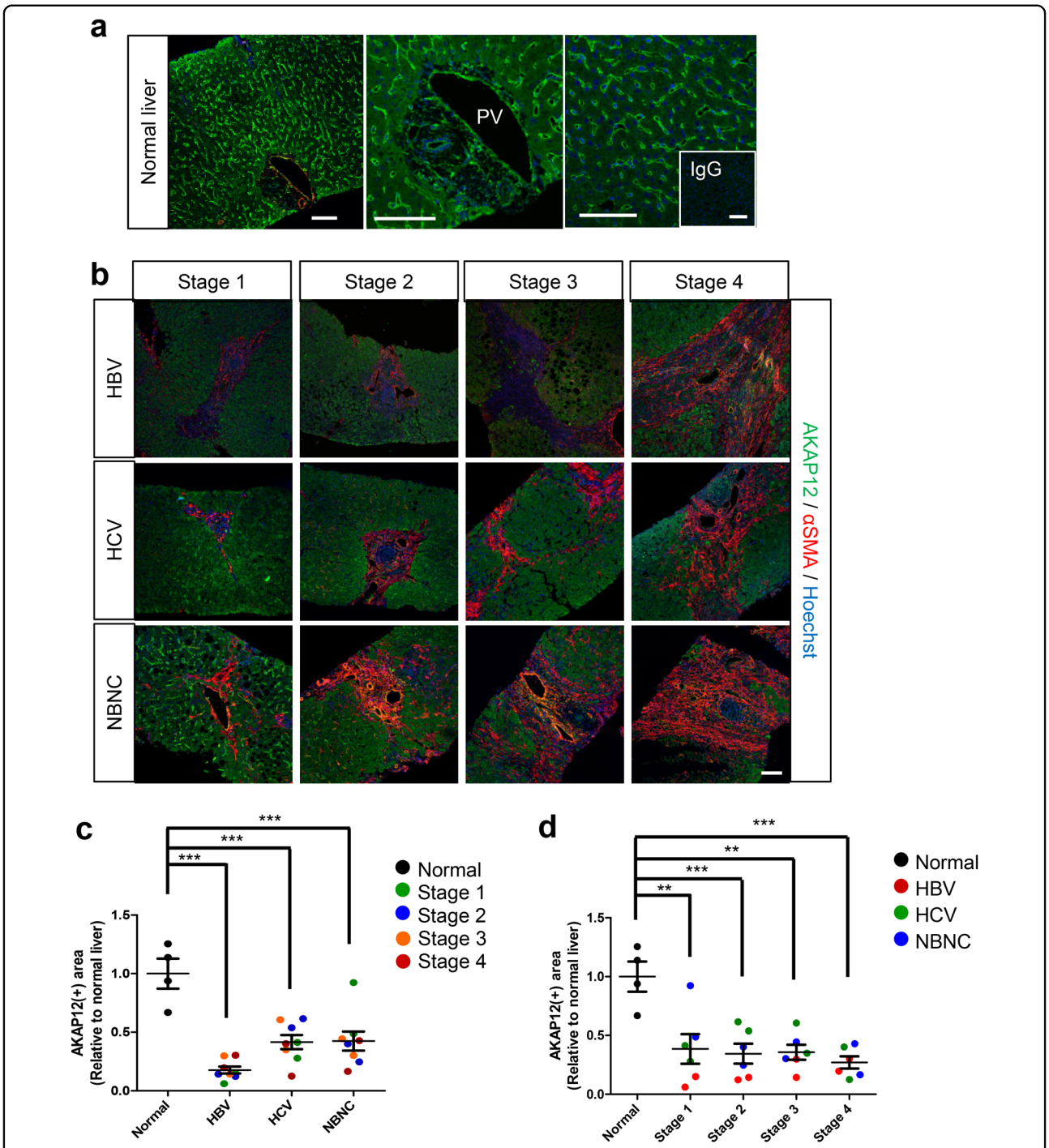

Fig. 2 AKAP12 is downregulated in fibrotic human livers. a Paraffin sections from normal liver biopsies were stained for AKAP12 (green) and αSMA (red). AKAP12 immunoreactivity was prominent in the portal tract (middle) and sinusoids (right). The inset within the last image to the right shows anti-rabbit IgG staining. Scale bars represent 100 μm. **b** Representative images of AKAP12 (green) and αSMA (red) staining on human liver specimens with fibrosis from stage 1 to 4 caused by hepatitis B virus (HBV, top row), hepatitis C virus (HCV, middle row), or non-HBV/non-HCV (NBNC, bottom row). Scale bar represents 100 μm. **c**, **d** Graphs represent relative AKAP12-positive area analyzed by etiologies (**c**) or fibrosis stages (**d**) ($n = 4$ in normal, $n = 8$ in each etiology group, $n = 6$ in each stage group). Data are expressed as the mean ± SEM. $^{**}P < 0.01$, $^{***}P < 0.001$

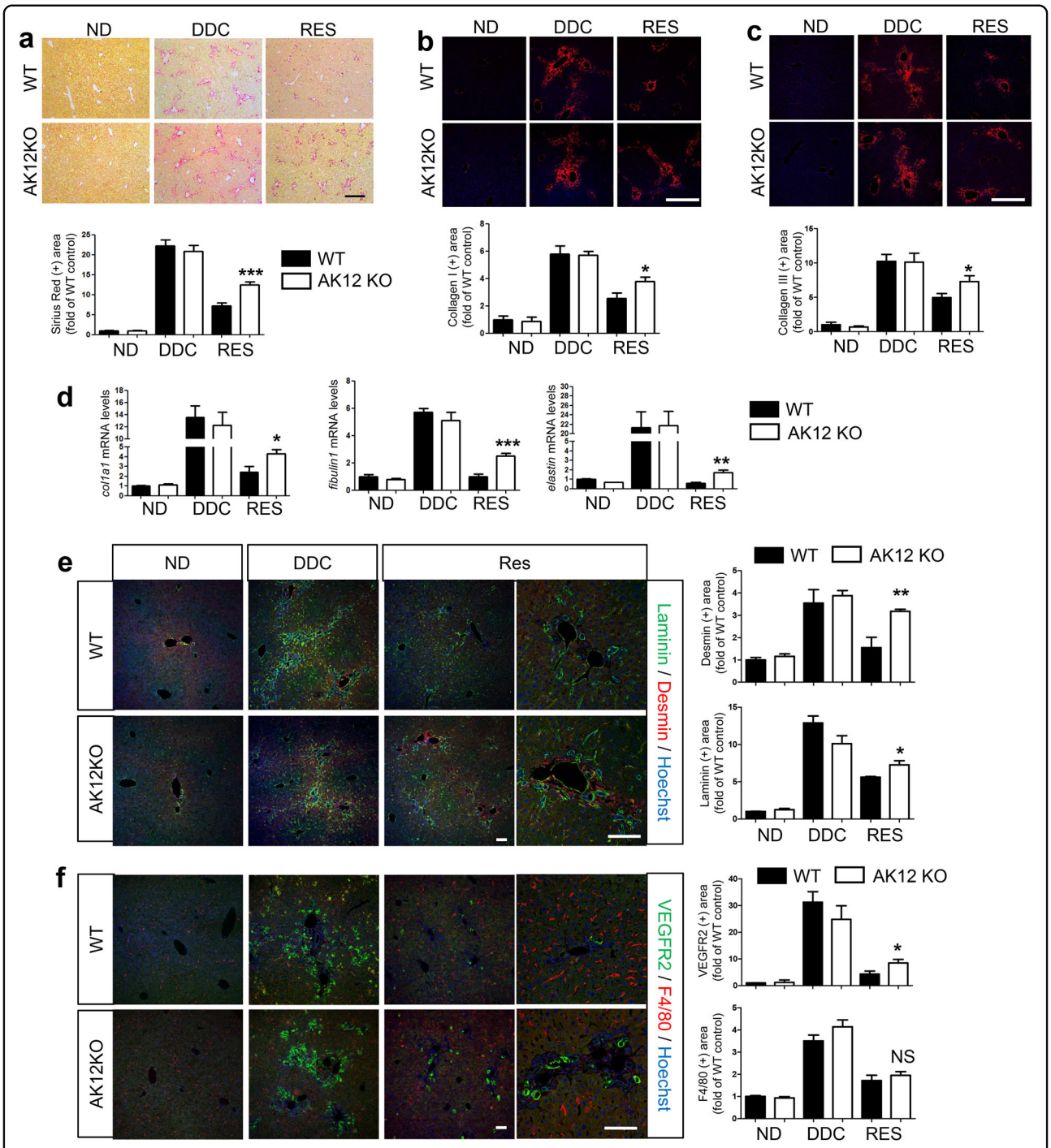

Fig. 3 AKAP12 KO mice display reduced fibrosis resolution accompanied by impaired reversion of activated myofibroblasts and vascular remodeling. a–**c** Liver sections from WT or AKAP12 KO mice fed a normal diet (ND), DDC-containing diet for 3 weeks (DDC), and DDC-containing diet for 3 weeks followed by a normal diet for 2 weeks (RES), which were stained with Sirius Red (**a**) and IHC against collagen I (**b**), and collagen III (**c**). Scale bars indicate 500 μm. Graphs are morphometric quantifications of areas stained by Sirius Red, collagen I, and collagen III. Data are expressed as the mean ± SEM. $n = 4$ mice for ND, $n = 10$ mice for DDC, $n = 11$–12 mice for RES (**a**). $n = 2$ mice for ND, $n = 5$ mice for DDC, $n = 5$–6 mice for RES (**b**, **c**). **d** Relative mRNA levels of Col1a1, Fibulin1, and Elastin in liver tissues were quantified by qPCR with specific primers. $n = 2$ mice for ND, $n = 5$ mice for DDC, $n = 5$ mice for RES. Data are expressed as the mean ± SEM. **e**, **f** Liver sections were subjected to IHC to detect laminin and desmin (**e**) or VEGFR2 and F4/80 (**f**). Scale bars indicate 100 μm. Graphs show relative areas positive for each type of staining. Data are expressed as the mean ± SEM. $n = 2$ mice for ND, $n = 5$ mice for DDC, $n = 5$–6 mice for RES. *$P < 0.05$; **$P < 0.01$; ***$P < 0.001$; NS not significant

Vascular remodeling was reversed as fibrosis resolved in WT mice. In AKAP12 KO mouse livers, however, VEGFR2-positive and laminin-positive staining was higher compared to that in WT mouse livers during fibrosis resolution (Fig. 3e, f), implying that the reversion of remodeled sinusoids to differentiated ones in AKAP12 KO mice is lower than that in WT mice. Although F4/80-positive myeloid cell populations increased during fibrosis and then reduced as fibrosis resolved, we did not observe significant differences in the number of these cells between WT and AKAP12 KO mice (Fig. 3f). Taken together, these results suggest that the reduced fibrosis resolution observed in AKAP12 KO mice is associated with impaired normalization of myofibroblasts and liver sinusoids.

Transcriptome analysis of WT and AKAP12 KO livers during fibrosis resolution

To investigate the molecular and cellular mechanisms underlying the positive effects of AKAP12 on fibrosis resolution, the transcriptomes of WT and AKAP12 KO livers during fibrosis resolution were analyzed by RNA sequencing (RNA-seq). Three mice were randomly selected from each genotype for RNA-seq analysis. A total of 1033 genes were found to be differentially expressed between the two genotypes with $P < 0.05$. Among these 1033 differentially expressed genes, 579 genes were upregulated in AKAP12 KO samples. In agreement with the results from immunohistochemical and quantitative polymerase chain reaction (qPCR) analyses, genes belonging to GO terms “extracellular matrix structural constituent,” “collagen binding”, and “extracellular matrix binding” were mostly elevated in AKAP12 KO samples (Fig. 4a, left). In addition, expression levels of genes belonging to the GO terms “positive regulation of angiogenesis” and “basement membrane” were also mostly elevated in AKAP12 KO samples (Fig. 4a, right). Molecular pathways, such as focal adhesion, GTPase-mediated signal transduction, and the adenosine 3′,5′-cyclic monophosphate (cAMP) signaling pathway, which can inhibit fibrosis[12], were predicted to be associated with impaired fibrosis resolution in AKAP12 KOs by Kyoto Encyclopedia of Genes and Genomes (KEGG) pathway (Fig. 4b) and GO analysis (Fig. 4c, d).

Role of AKAP12 in activation of PFs and association with cAMP pathway

In accordance with the RNA sequencing results, qPCR revealed that transcript levels of PDE4a (a member of the PDE4 family of proteins that hydrolyze cAMP) were elevated in AKAP12 KOs during fibrosis resolution (Fig. 5a). It was previously demonstrated that forskolin, a cAMP activator, attenuated CCL4-induced liver fibrosis in a rodent model[9]. Moreover, rolipram, a PDE4 inhibitor, attenuated bile-duct ligation (BDL)-induced fibrosis in rats[33], implying that the cAMP signaling pathway has an inhibitory role in hepatic fibrosis. Consistent with these in vivo studies, treatment of primary cultures of mouse PFs with forskolin significantly reduced the expression of myofibroblast-related genes (Fig. 5b). The inhibitory effect of forskolin on Col1a1, Col15a1, and Elastin gene expression was reversed by co-treatment with a PKA inhibitor, H89, whereas the expression levels of Col3a1 and αSMA were unaffected by PKA inhibition (Fig. 5b); this result means that increased cAMP levels induced by forskolin resulted in the inhibition of myofibroblastic gene expression, which is mediated in part through the activation of PKA.

On the basis of the association of AKAP12 with the cAMP pathway[18] and the inhibitory effect of cAMP signaling on myofibroblast activation, we hypothesized that AKAP12 may have an inhibitory role in hepatic fibrosis via modulation of the cAMP pathway. We then examined the role of AKAP12 in regulating the myofibroblastic activation of PFs in a cell-intrinsic manner. Mouse primary PFs were transfected with either control siRNA or AKAP12 siRNA, following which the expression profiles of key myofibroblast marker genes were measured by qPCR. Although the levels of αSMA were comparable, AKAP12 knockdown PFs expressed more Col1a1, Col3a1, Col15a1, and Elastin than controls (Fig. 5c). These effects were, however, abolished by rolipram treatment (Fig. 5d), indicating that AKAP12 knockdown led to the activation of PDE4-mediated cAMP hydrolysis. These results indicate that AKAP12 inhibits the activation of PFs and that this effect is probably associated with its function as a scaffold protein in the cAMP signaling pathway.

Role of AKAP12 in sinusoidal remodeling

Soluble factors are believed to mediate the crosstalk between liver sinusoids and hepatocytes or other non-parenchymal cells[34,35]. To identify the factor(s) that could mediate the effects of AKAP12 on vascular remodeling, we measured levels of various angiocrine factors. We found that in AKAP12 KO livers, the levels of endothelin-1 (ET-1) are upregulated during fibrosis resolution, whereas the levels of hepatocyte growth factor (HGF), wingless-type MMTV integration site family member 2 (Wnt2), and vascular endothelial growth factor (VEGF) were comparable to those in the livers of WT littermates (Fig. 6a). Interestingly, serum levels of ET-1 were also elevated in AKAP12 KO mice, not only during fibrosis resolution but also under normal conditions (Fig. 6b). To test whether AKAP12 inhibits vascular remodeling by directly regulating LSECs, human primary LSECs (hLSECs) were transfected with siRNAs against AKAP12, following which the expression levels of basement membrane components and the angiogenic capacity of cells

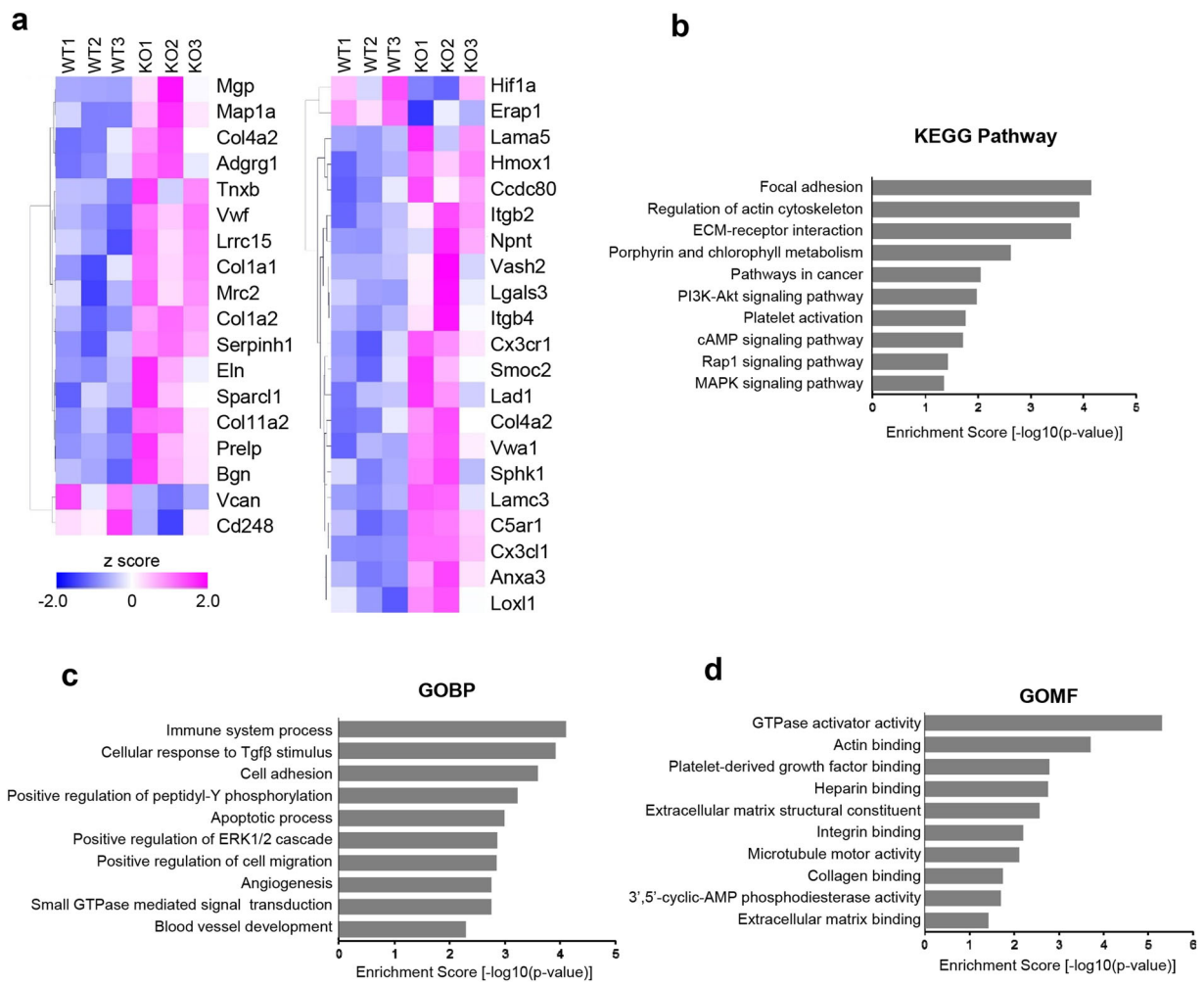

Fig. 4 Transcriptome analysis of WT and AKAP12 KO livers at resolution state. a Heatmap of differentially expressed genes belong to GO terms "extracellular matrix structural constituent," "collagen binding", and "extracellular matrix binding" (left) and "positive regulation of angiogenesis" and "basement membrane" (right) showing differences in gene expression levels between WT and AKAP12 KO samples. Each row represents one gene, and each column represents one sample. The scale bar indicates row *z*-scores of gene expression values, with highly expressed genes depicted in pink and genes with low-level expression depicted in blue. Cluster analysis of the gene expression data was performed to group genes with similar expression patterns across experimental conditions. **b** Enrichment analysis of the KEGG pathway assignments of genes potentiated in AKAP12 KO livers. **c** Enrichment analysis of gene ontology biological processes (GOBP) of genes modulated in AKAP12 KO livers. **d** Gene ontology analysis for molecular function (GOMF) of genes modulated in AKAP12 KO livers

were measured. Among the laminins, Laminin α1 and α5 were upregulated by AKAP12 knockdown (Fig. 6c), suggesting that AKAP12 is involved in basement membrane reconstitution. Furthermore, AKAP12 knockdown in hLSECs increased ET-1 gene expression (Fig. 6c) and caused the formation of tube-like structures (Fig. 6d). These results suggest that in LSECs, AKAP12 inhibits basement membrane formation, ET-1 expression, and angiogenesis in a cell-intrinsic manner. To verify the negative relationship between AKAP12 expression and sinusoidal remodeling, we analyzed a publicly available microarray data set (GSE1843) on liver endothelial cells (LECs) isolated from rat livers with or without CCL4-induced cirrhosis[36]. The data indicated that levels of AKAP12 mRNA were significantly decreased in cirrhotic LECs and negatively correlated with levels of ET-1 or Laminin α5 transcripts (Fig. 6e). Therefore, it is likely that reduced AKAP12 expression levels during fibrogenesis promote sinusoidal remodeling, whereas restoration of AKAP12 expression during fibrosis resolution accelerates the recovery of normal sinusoidal characteristics.

Discussion

As liver fibrosis can be naturally reversed by removing injury-causing agents, understanding the precise mechanisms mediating fibrosis resolution can provide

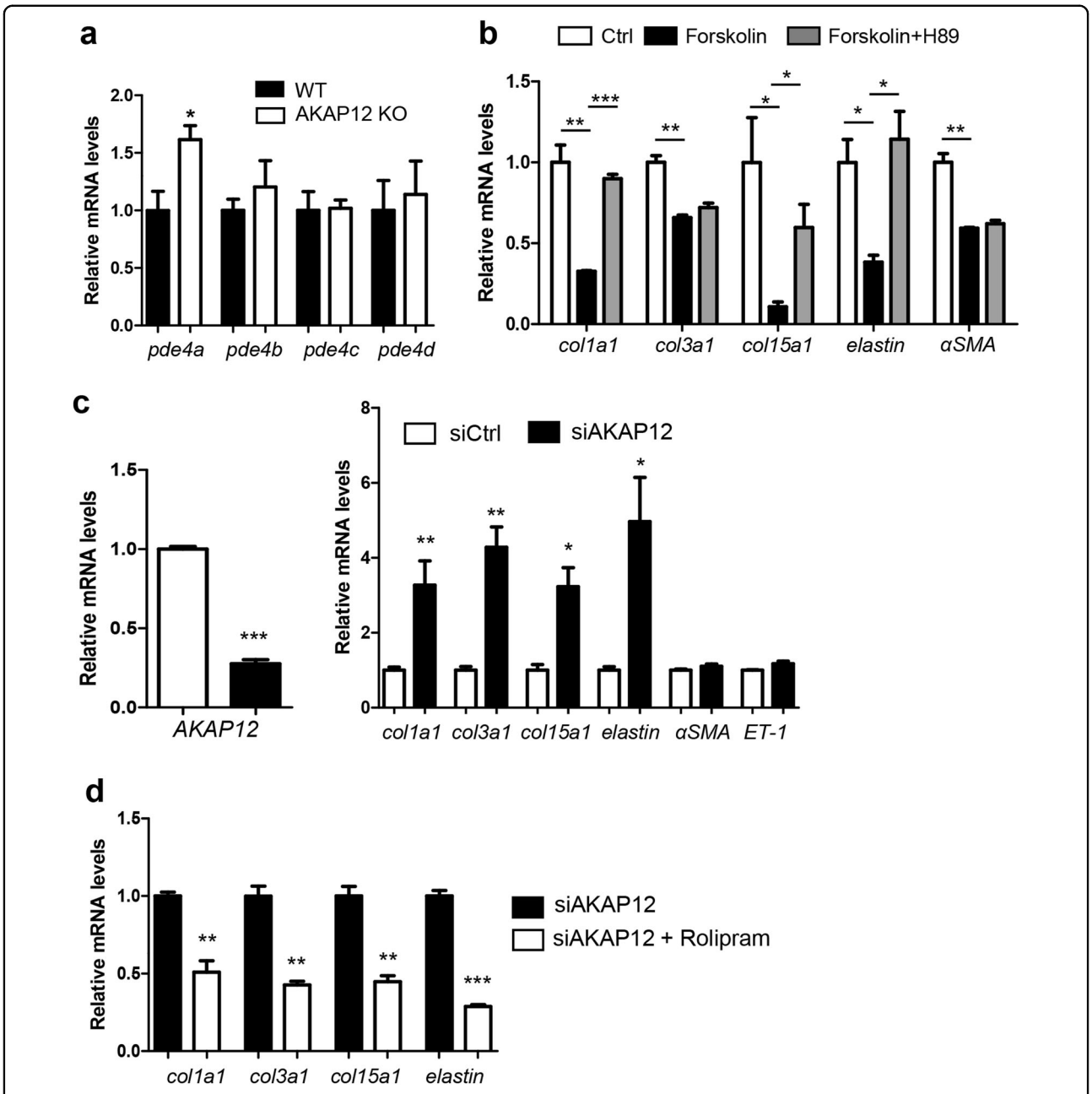

Fig. 5 AKAP12 inhibits activation of PFs in association with the cAMP signaling pathway. a qPCR of liver tissue during fibrosis resolution showing relative mRNA levels of gene members of the PDE4 family ($n = 6$ mice per genotype). **b** Primary mouse PFs were treated with either forskolin (10 μM) alone or with a combination of forskolin (10 μM) and H89 (10 μM) for 16 h. Relative mRNA levels of Col1a1, Col3a1, Col15a1, Elastin, and αSMA were measured by qPCR with specific primers. $n = 3$ for each group. **c**, **d** Mouse PFs were transfected with control or AKAP12 siRNAs. Graphs show mRNA expression levels of AKAP12 and myofibroblast-related genes in siAKAP12-treated PFs relative to those in control siRNA-treated PFs (siCtrl) (**c**). PFs transfected with siAKAP12 were treated with rolipram (20 μM) for 24 h, and the relative levels of ECM gene expression were measured by qPCR (**d**). $n = 3$ repeats. Data are expressed as the means ± SEM. $^{*}P < 0.05$; $^{**}P < 0.01$; $^{***}P < 0.001$

new therapeutic strategies for fibrosis treatment. In this study, we identified AKAP12 as a key molecule that promotes fibrosis resolution. AKAP12 expression in both PFs and LSECs was downregulated during fibrogenesis but was restored during fibrosis resolution. Reduction in AKAP12 expression levels during liver fibrosis was not only observed in a mouse model but was also observed in human liver tissues exhibiting various stages of fibrosis caused by different etiologies. AKAP12 KO mice displayed reduced fibrosis resolution in association with

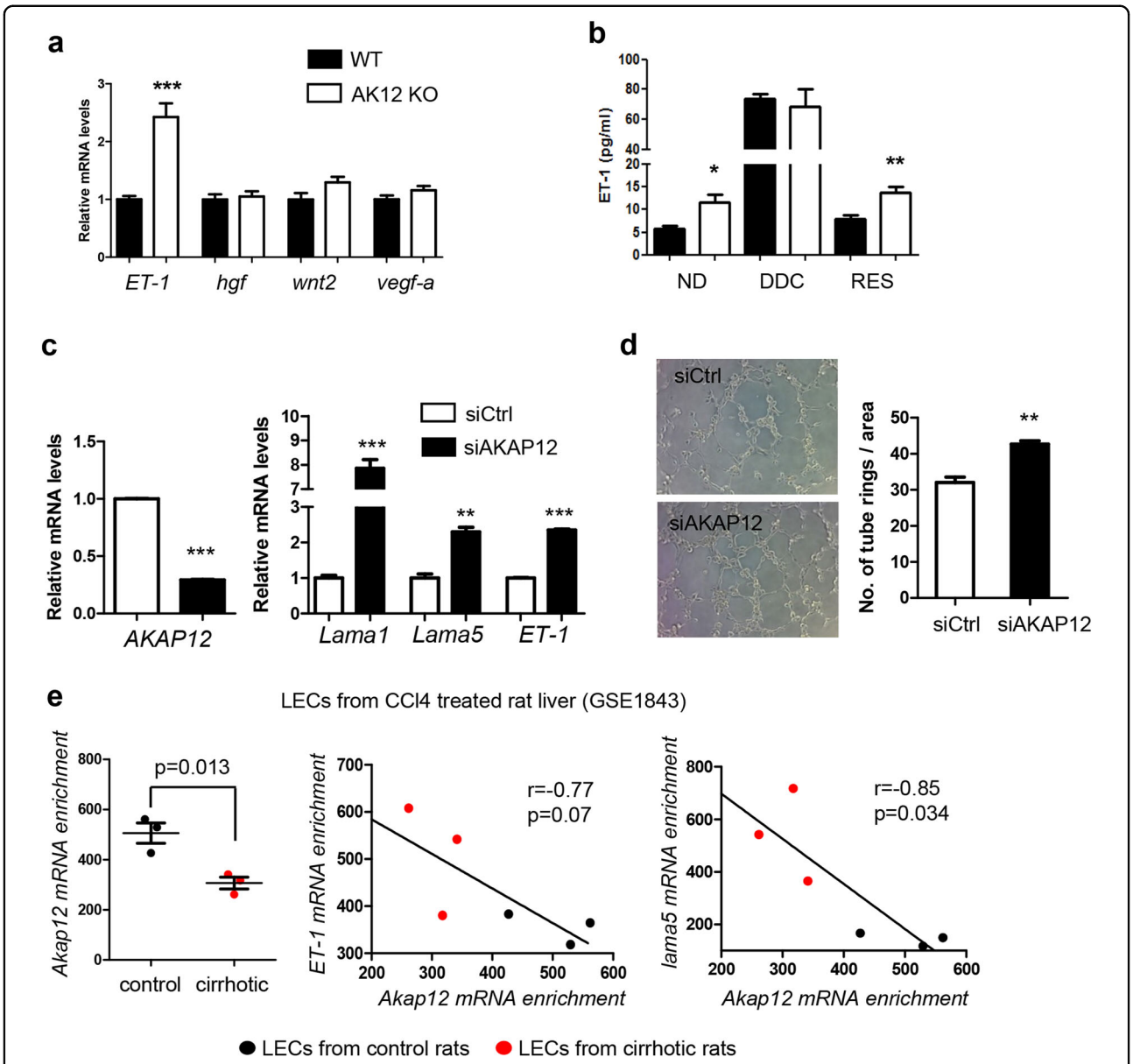

Fig. 6 AKAP12 deficiency leads to ET-1 gene expression, laminin reconstitution, and angiogenesis of LSECs. a qPCR of liver tissue during fibrosis resolution revealed increased expression of ET-1 in AKAP12 KO mice ($n = 5$ mice per genotype). **b** Serum levels of ET-1 measured by ELISA from WT or AKAP12 KO mice ($n = 3$ mice in ND groups, $n = 5$ mice in DDC groups, $n = 6$ mice in RES groups). **c** hLSECs were transfected with control or AKAP12 siRNAs, following which relative mRNA levels were measured by qPCR. Note that AKAP12 knockdown resulted in increased expression of Laminin α1 (lama1), Laminin α5 (lama5), and ET-1 ($n = 3$ repeats). **d** Matrigel tube formation assays on hLSECs show an increased number of tube rings in AKAP12 knockdowns ($n = 3$ repeats). Data are expressed as the mean ± SEM. $^{*}P < 0.05$; $^{**}P < 0.01$; $^{***}P < 0.001$. **e** An analysis of GEO data set GSE1843 showing significant reduction in AKAP12 in liver endothelial cells (LECs) isolated from cirrhotic rats (left graph). Pearson correlation of AKAP12 levels and ET-1 (middle graph) or lama5 (right graph) levels shows negative correlation values ($n = 3$ samples per group)

myofibroblast and endothelial characteristics, implying that recovery of AKAP12 expression is required for proper normalization of portal fibroblasts and liver sinusoids during fibrosis resolution.

Dynamic alteration of AKAP12 expression during fibrosis onset and resolution suggests that its expression can be regulated by microenvironmental factors. Our group previously reported that retinoic acid (RA) and TGF-β1 can induce AKAP12 expression to mediate epithelial-to-mesenchymal transition in meningeal reconstruction; however, this effect was abolished by local hypoxia[21]. We have also shown that during central nervous system (CNS) vascular development, AKAP12 expression is decreased due to hypoxia during active

angiogenesis but can be restored through reoxygenation[20]. Interestingly, TGF-β1 is a potent inducer of hepatic fibrosis, and the liver is a retinol-rich organ that takes up ~70% of dietary retinol[37]. Moreover, several lines of evidence indicate that tissue hypoxia occurs during hepatic fibrosis and that hypoxia-mediated signaling affects a wide array of cellular responses, such as myofibroblast activation, angiogenesis, and immune responses[38–40]. Therefore, it is possible that these microenvironmental factors modulate AKAP12 expression in hepatic fibrosis.

RNA sequencing analysis strongly suggested that the antifibrogenic role of AKAP12 is associated with the cAMP pathway. Indeed, members of the AKAP family are scaffold proteins that fine-tune cAMP signaling through spatio-temporal regulation[18]. AKAP12 is mostly localized to the plasma membrane, where it mediates the subcellular compartmentalization of cAMP[19]. cAMP is a second messenger in the G-protein-coupled receptor (GPCR) signal cascade that regulates a wide range of cellular responses. Reports indicate that in liver fibrosis, either direct activation of cAMP signaling by forskolin[12] or inhibition of the cAMP-hydrolyzing enzyme PDE4[33] attenuated fibrogenesis in animal models; this finding suggests that boosting cAMP signaling could have therapeutic value in treating liver fibrosis. Nevertheless, stimulating cAMP signaling directly has limited therapeutic value due to unacceptable side effects caused by its broad-range effects on numerous cellular processes[41]. In this regard, using AKAP12 to stimulate cAMP signaling could provide new therapeutic approaches that minimize undesirable side effects.

In conclusion, our results suggest that AKAP12, whose expression is dynamically altered during fibrosis onset and resolution, has a central role in the proper resolution of liver fibrosis.

Acknowledgements
This work was supported by the Global Research Laboratory Program (2011-0021874), the Global Core Research Center (GCRC) Program (2011-0030001), Bio & Medical Technology Development Program (2015M3A9E6028949), NRF grant (2015R1C1A2A01054446 to H.S.L.), and Basic Science Research Program (NRF-2017R1A6A3A11032239 to S.-J.B.) through the National Research Foundation of Korea (NRF) funded by the Ministry of Education, Ministry of Science, ICT and Future Planning (MSIP).

Author details
[1]College of Pharmacy and Research, Institute of Pharmaceutical Sciences Seoul National University Seoul 08826, Korea. [2]Department of Biochemistry, School of Medicine, Keimyung University, Daegu 42601, Korea. [3]Department of Internal Medicine, Inje University College of Medicine, Seoul Paik Hospital, Seoul, Korea. [4]Department of Internal Medicine, University of Ulsan College of Medicine, Asan Medical Center, Seoul, Korea. [5]Department of Internal Medicine, Hallym University College of Medicine, Kangdong Sacred Heart Hospital, Seoul, Korea. [6]Department of Pathology, University of Ulsan College of Medicine, Asan Medical Center, Seoul, Korea. [7]Crop Biotechnology Institute, GreenBio Science and Technology, Seoul National University, Pyeongchang 25354, Korea

Conflict of interest
The authors declare that they have no conflict of interest.

Supplementary information accompanies this paper at https://doi.org/10.1038/s12276-018-0074-5.

Received: 16 January 2018 Revised: 20 February 2018 Accepted: 22 February 2018.
Published online: 27 April 2018

References

1. Pellicoro, A., Ramachandran, P., Iredale, J. P. & Fallowfield, J. A. Liver fibrosis and repair: immune regulation of wound healing in a solid organ. *Nat. Rev. Immunol.* **14**, 181–194 (2014).
2. Friedman, S. L. Mechanisms of hepatic fibrogenesis. *Gastroenterology* **134**, 1655–1669 (2008).
3. Zoubek, M. E., Trautwein, C. & Strnad, P. Reversal of liver fibrosis: from fiction to reality. *Best Pract. Res. Clin. Gastroenterol.* **31**, 129–141 (2017).
4. Sun, M. & Kisseleva, T. Reversibility of liver fibrosis. *Clin. Res. Hepatol. Gastroenterol.* **39**(Suppl 1), S60–S63 (2015).
5. Dranoff, J. A. & Wells, R. G. Portal fibroblasts: underappreciated mediators of biliary fibrosis. *Hepatology* **51**, 1438–1444 (2010).
6. Issa, R. et al. Apoptosis of hepatic stellate cells: involvement in resolution of biliary fibrosis and regulation by soluble growth factors. *Gut* **48**, 548–557 (2001).
7. Krizhanovsky, V. et al. Senescence of activated stellate cells limits liver fibrosis. *Cell* **134**, 657–667 (2008).
8. Troeger, J. S. et al. Deactivation of hepatic stellate cells during liver fibrosis resolution in mice. *Gastroenterology* **143**, 1073–1083 (2012). e1022.
9. Fabregat, I. et al. TGF-beta signalling and liver disease. *FEBS J.* **283**, 2219–2232 (2016).
10. Bonner, J. C. Regulation of PDGF and its receptors in fibrotic diseases. *Cytokine Growth Factor Rev.* **15**, 255–273 (2004).
11. Zardi, E. M. et al. Hepatic PPARs: their role in liver physiology, fibrosis and treatment. *Curr. Med Chem.* **20**, 3370–3396 (2013).
12. El-Agroudy, N. N., El-Naga, R. N., El-Razeq, R. A. & El-Demerdash, E. Forskolin, a hedgehog signalling inhibitor, attenuates carbon tetrachloride-induced liver fibrosis in rats. *Br. J. Pharmacol.* **173**, 3248–3260 (2016).
13. Lopez-Sanchez, I. et al. GIV/Girdin is a central hub for profibrogenic signalling networks during liver fibrosis. *Nat. Commun.* **5**, 4451 (2014).
14. DeLeve, L. D. Liver sinusoidal endothelial cells in hepatic fibrosis. *Hepatology* **61**, 1740–1746 (2015).
15. Iwakiri, Y., Shah, V. & Rockey, D. C. Vascular pathobiology in chronic liver disease and cirrhosis—current status and future directions. *J. Hepatol.* **61**, 912–924 (2014).
16. Deleve, L. D., Wang, X. & Guo, Y. Sinusoidal endothelial cells prevent rat stellate cell activation and promote reversion to quiescence. *Hepatology* **48**, 920–930 (2008).
17. Xie, G. et al. Role of differentiation of liver sinusoidal endothelial cells in progression and regression of hepatic fibrosis in rats. *Gastroenterology* **142**, 918–927.e916 (2012).
18. Poppinga, W. J., Munoz-Llancao, P., Gonzalez-Billault, C. & Schmidt, M. A-kinase anchoring proteins: cAMP compartmentalization in neurodegenerative and obstructive pulmonary diseases. *Br. J. Pharmacol.* **171**, 5603–5623 (2014).
19. Tao, J. & Malbon, C. C. G-protein-coupled receptor-associated A-kinase anchoring proteins AKAP5 and AKAP12: differential signaling to MAPK and GPCR recycling. *J. Mol. Signal.* **3**, 19 (2008).
20. Lee, S. W. et al. SSeCKS regulates angiogenesis and tight junction formation in blood-brain barrier. *Nat. Med.* **9**, 900–906 (2003).
21. Cha, J. H. et al. Prompt meningeal reconstruction mediated by oxygen-sensitive AKAP12 scaffolding protein after central nervous system injury. *Nat. Commun.* **5**, 4952 (2014).
22. Cha, J. H. et al. AKAP12 mediates barrier functions of fibrotic scars during CNS repair. *PLoS ONE* **9**, e94695 (2014).

23. Gelman, I. H. Suppression of tumor and metastasis progression through the scaffolding functions of SSeCKS/Gravin/AKAP12. *Cancer Metastasis Rev.* **31**, 493–500 (2012).
24. Goeppert, B. et al. Down-regulation of tumor suppressor A kinase anchor protein 12 in human hepatocarcinogenesis by epigenetic mechanisms. *Hepatology* **52**, 2023–2033 (2010).
25. Akakura, S., Huang, C., Nelson, P. J., Foster, B. & Gelman, I. H. Loss of the SSeCKS/Gravin/AKAP12 gene results in prostatic hyperplasia. *Cancer Res.* **68**, 5096–5103 (2008).
26. El Mourabit, H., Loeuillard, E., Lemoinne, S., Cadoret, A. & Housset, C. Culture model of rat portal myofibroblasts. *Front. Physiol.* **7**, 120 (2016).
27. Dobin, A. et al. STAR: ultrafast universal RNA-seq aligner. *Bioinformatics* **29**, 15–21 (2013).
28. Trapnell, C. et al. Transcript assembly and quantification by RNA-Seq reveals unannotated transcripts and isoform switching during cell differentiation. *Nat. Biotechnol.* **28**, 511–515 (2010).
29. Trapnell, C. et al. Differential analysis of gene regulation at transcript resolution with RNA-seq. *Nat. Biotechnol.* **31**, 46–53 (2013).
30. Huang da, W., Sherman, B. T. & Lempicki, R. A. Systematic and integrative analysis of large gene lists using DAVID bioinformatics resources. *Nat. Protoc.* **4**, 44–57 (2009).
31. Subramanian, A. et al. Gene set enrichment analysis: a knowledge-based approach for interpreting genome-wide expression profiles. *Proc. Natl Acad. Sci. USA* **102**, 15545–15550 (2005).
32. Xu, M., Wang, X., Zou, Y. & Zhong, Y. Key role of liver sinusoidal endothelial cells in liver fibrosis. *Biosci. Trends* **11**, 163–168 (2017).
33. Gobejishvili, L. et al. Rolipram attenuates bile duct ligation-induced liver injury in rats: a potential pathogenic role of PDE4. *J. Pharmacol. Exp. Ther.* **347**, 80–90 (2013).
34. Kostallari, E. & Shah, V. H. Angiocrine signaling in the hepatic sinusoids in health and disease. *Am. J. Physiol. Gastrointest. Liver Physiol.* **311**, G246–G251 (2016).
35. Ding, B. S. et al. Divergent angiocrine signals from vascular niche balance liver regeneration and fibrosis. *Nature* **505**, 97–102 (2014).
36. Tugues, S. et al. Microarray analysis of endothelial differentially expressed genes in liver of cirrhotic rats. *Gastroenterology* **129**, 1686–1695 (2005).
37. Shirakami, Y., Lee, S. A., Clugston, R. D. & Blaner, W. S. Hepatic metabolism of retinoids and disease associations. *Biochim. Biophys. Acta* **1821**, 124–136 (2012).
38. Wang, J. et al. Reduction of hepatic fibrosis by overexpression of von Hippel-Lindau protein in experimental models of chronic liver disease. *Sci. Rep.* **7**, 41038 (2017).
39. Roth, K. J. & Copple, B. L. Role of hypoxia-inducible factors in the development of liver fibrosis. *Cell Mol. Gastroenterol. Hepatol.* **1**, 589–597 (2015).
40. Copple, B. L., Kaska, S. & Wentling, C. Hypoxia-inducible factor activation in myeloid cells contributes to the development of liver fibrosis in cholestatic mice. *J. Pharmacol. Exp. Ther.* **341**, 307–316 (2012).
41. Dema, A., Perets, E., Schulz, M. S., Deak, V. A. & Klussmann, E. Pharmacological targeting of AKAP-directed compartmentalized cAMP signalling. *Cell Signal.* **27**, 2474–2487 (2015).